

**FABRICATION OF TITANIA AND CARBON NITRIDE
BASED THIN FILM ELECTRODES FOR
PHOTOELECTROCHEMICAL WATER SPLITTING**

RAVI TEJASVI



**DEPARTMENT OF CHEMICAL ENGINEERING
INDIAN INSTITUTE OF TECHNOLOGY DELHI**

OCTOBER 2020

© Indian Institute of Technology Delhi (IITD), New Delhi, 2020

**FABRICATION OF TITANIA AND CARBON NITRIDE
BASED THIN FILM ELECTRODES FOR
PHOTOELECTROCHEMICAL WATER SPLITTING**

by

RAVI TEJASVI

Department of Chemical Engineering

Submitted

in fulfilment of the requirements of the degree of Doctor of Philosophy

to the

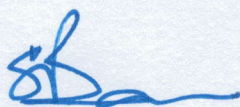


INDIAN INSTITUTE OF TECHNOLOGY DELHI

OCTOBER 2020

Certificate

It is to certify that the thesis titled '**Fabrication of Titania and Carbon Nitride based Thin Film Electrodes for Photoelectrochemical Water Splitting**' being submitted by **Ravi Tejasvi** to the Indian Institute of Technology Delhi, for fulfilment of the requirements for the award of **Doctor of Philosophy in Chemical Engineering** is a record of bonafide research work carried out by him. He has worked under my supervision and has fulfilled the requirements, which, to my knowledge, has reached the requisite standard for the submission of the thesis. The research report and results presented in this thesis have not been submitted, in part or full, to any other university or institute for the award of any degree or diploma.



Siddhasatwa Basu

Professor,

Department of Chemical Engineering

Indian Institute of Technology Delhi

Hauz Khas, New Delhi-110016

Acknowledgements

This thesis, my research work, and my achievements are there because, on May 16, 2014, Prof. Suddhasatwa Basu accepted me as his prospective Ph.D. student. The significance of Prof. Basu to this work and me can be best described by this short story:

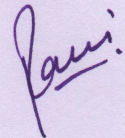
Once there was a rabbit, sitting outside his burrow, typing on his laptop. "What are you working on?" asked a fox. "My thesis," replied the rabbit. "Hmm, what is it about?" enquired the fox. "on how rabbits eat foxes," answered the rabbit. "That's ridiculous! Rabbits don't eat foxes!" exclaimed the fox. Rabbit calmly replied, "Come with me, and I'll show you." They both disappeared into the rabbit's burrow, and after a few minutes, gnawing on a fox bone, rabbit returned to his laptop and resumed typing. Soon came a wolf who asked the same question and met a similar fate. Then came a bear and asked, "What are you doing?" Rabbit: "I'm doing a thesis on how rabbits eat bears." Bear: "Well, that's absurd!" Rabbit: "Come into my home, and I'll show you." They both went inside the rabbit's burrow. In one corner, there was a pile of fox bones. In another corner lay a pile of wolf bones. On the other side of the room, a huge lion was belching and picking his teeth. MORAL: It does not matter what you choose for a thesis topic. It does not matter what you use for your data. It does not even matter if your topic makes sense. What matters is whom you have for a thesis advisor.

I am indebted to my scholar research committee members, Prof. Anupam Shukla, Prof. Anil Verma, and Prof. Bodhraj Mehta, who could always find time to advise me despite their tightly packed schedules. I am blessed that I could have a few enlightening conversations with Prof. Ashok Gupta. I humbly acknowledge the help I got from Prof. Rajesh Khanna, Prof. Kamal K. Pant, and Prof. Shalini Gupta in the matters crucial to me as a research scholar.

At this juncture, I admit that the journey would have been unbearable if I had not had the company of Baijnath. We were the passenger of the same boat, and I am glad we are completing the journey together. I also much enjoyed many laughs with Dr. Aadesh P. Singh, Dr. Nimai

Bhandary, Dr. Harikrishnan, and Dr. Pankaj Tiwari. My research work relied greatly on the support from Shahid, Aditya, Mohit, Ramji, Biswajit, and all the members of the Fuel Cell Lab. It would not be exaggerating to say that Mr. Sundar Singh Kasana, was *the consigliere* and the glue keeping *the FC Lab family* together.

My parents, Smt. Chandravati Bajpai and Sh. Awadh Bihari Bajpai, personify God to me. My sister, Sonam, is the polestar of my life. It is my daughter Aadya who keeps me lively in the most testing times. Finally, there is this person who did not lose me even when I felt having lost myself somewhere. Upasana, my dear wife, I dedicate this thesis to you and your patience.



Ravi Tejasvi

Abstract

Renewable and clean energy is the global need of the hour, and the hydrogen economy is the way to meet it. Out of all the currently practiced and prospective technologies of hydrogen generation, photoelectrochemical water splitting technology is the most efficient technology because it needs only sunlight to split water into hydrogen and oxygen over a designed catalytic surface. The photoactivity is the most critical feature of the catalyst because it controls the rate and efficiency of the water splitting process. The photoactivity of the catalyst can be enhanced either by designing a new material or by redesigning the existing methods of using the known materials. The presented thesis identifies three new ways of enhancing the photoactivity of the already known $\text{TiO}_2/\text{C}_3\text{N}_4$ heterojunction catalyst in the photoelectrochemical water splitting.

A simple method for depositing a thin film of two-dimensional exfoliated carbon nitride (eC_3N_4) nanoflakes on a substrate using a centrifugation technique has been developed, whereby solvent evaporation is prevented, and solvent reuse is possible. The centrifuge technique of deposition yields uniform, smooth thin film irrespective of substrate surface texture. The deposited $\text{TiO}_2/\text{eC}_3\text{N}_4$ film studied, through a scanning electron microscope (SEM), atomic force microscope (AFM), and optical surface profilometer, shows a variation in surface roughness based on centrifugation speeds. Initially, film coverage improves, and surface roughness decreases with the increase in rotational speed of the centrifuge, and the surface roughness slightly increases with further increase in the rotational speed. The photoelectrochemical (PEC) studies of $\text{TiO}_2/\text{eC}_3\text{N}_4$ films, including linear sweep voltammetry (LSV) and electrochemical impedance spectroscopy (EIS), suggest that the centrifuge technique forms better heterojunctions compared to that by spin coating technique leading to enhanced PEC water splitting.

To eliminate the use of a solvent in depositing C_3N_4 thin films, a new approach that deposits stoichiometric C_3N_4 thin films through radio frequency magnetron (RFM) sputtering using pelletized gC_3N_4 powder as the sputtering target has been discovered. Thin-film samples are deposited on different substrates under Ar and N_2 as plasma media for different durations. These samples are analyzed by SEM, transmission electron microscopy (TEM), AFM, X-ray diffraction analysis (XRD), X-ray photoelectron spectroscopy (XPS), photoluminescence spectroscopy (PL), Raman spectroscopy, and PEC studies including chopped light voltammetry, incident photo-to-current conversion efficiency, and EIS. The use of Ar as the plasma medium allows the formation of a thin film of stoichiometrically conservative C_3N_4 in the TiO_2/C_3N_4 heterojunction sample. The PEC and PL studies concluded that the TiO_2/C_3N_4 heterojunction formed under Ar plasma offered a higher current density and lower impedance as compared to that offered by the TiO_2/C_3N_4 heterojunction formed under N_2 plasma. It signifies the beneficial use of compressed C_3N_4 as the sputtering target to form a stoichiometric and photoactive C_3N_4 thin film without the difficulty in controlling the N_2 gas flow rate with graphite as the target in the sputtering process. Moreover, the sputtering process does not require the formation of any dispersion for thin film deposition, and therefore the need for solvent in thin film deposition is eliminated.

To enhance the contact area between the substrate TiO_2 nanostructure and the sensitizer C_3N_4 thin films, a stemmed nanoflower structure of TiO_2 has been synthesized. The TiO_2 nanoflower array linking to stem on a Ti foil is synthesized by thermochemical digestion of titanium at 80 °C by hydrogen peroxide and hydrofluoric acid solution. TiO_2 nanoflower comprises the anatase TiO_2 , which encases the Ti metal core as seen by TEM, XRD, XPS based depth profile, and energy dispersive X-ray based elemental mapping. The physical analyses of air annealed samples verify the prominent presence of anatase (101) and anatase (200) crystals of about 35 nm size. The photoactivity of TiO_2/eC_3N_4 heterojunctions in PEC water splitting has been

assessed for the heterojunction formed by the TiO₂ nanoflower with C₃N₄, and the same is compared with the heterojunction of TiO₂ nanotubular array and C₃N₄. It has been found from LSV and EIS that the TiO₂/eC₃N₄ heterojunction formed by the synthesized stemmed-nanoflower of TiO₂ offers superior PEC activity towards water splitting as compared to the one formed by TiO₂ nanotubes. A method to recover the spent hydrofluoric acid from effluents of the thermochemical method has also been identified.

सार

अक्षय और स्वच्छ ऊर्जा विश्व की सामयिक आवश्यकता है और हाइड्रोजन अर्थव्यवस्था इसे पूरा करने का तरीका है। हाइड्रोजन उत्पादन के सभी वर्तमान में प्रचलित और भावी तकनीकों में से प्रकाश विद्युत रासायनिक जल विभाजन तकनीक सबसे कुशल तकनीक है क्योंकि इसे एक संरचित उत्प्रेरक सतह पर हाइड्रोजन और ऑक्सीजन में पानी को विभाजित करने के लिए केवल सूर्य के प्रकाश की आवश्यकता होती है। प्रकाशिक सक्रियता उत्प्रेरक की सबसे महत्वपूर्ण विशेषता है क्योंकि यह जल विभाजन प्रक्रिया की दर और दक्षता को नियंत्रित करता है। उत्प्रेरक की प्रकाशिक सक्रियता या तो एक नए पदार्थ को रचना करके या ज्ञात सामग्रियों के उपयोग के मौजूदा तरीकों को फिर से पुनः संरचित करके बढ़ाया जाता है। प्रस्तुत शोध प्रबंध प्रकाश विद्युत रासायनिक जल विभाजन में पहले से ही ज्ञात $\text{TiO}_2/\text{C}_3\text{N}_4$ हेटेरोजंक्शन उत्प्रेरक की प्रकाशिक सक्रियता को बढ़ाने के तीन नए तरीकों की पहचान करता है।

एक अपकेंद्रित तकनीक का उपयोग कर एक सबस्ट्रेट पर द्विआयामी एक्सफ़ोलीएटेड कार्बन नाइट्राइड (eC_3N_4) की एक पतली फिल्म जमा करने के लिए एक सरल विधि विकसित की गई है, जिससे विलायक वाष्पीकरण को रोका जाता है, और विलायक का पुनः उपयोग संभव है। अपसरण की अपकेंद्रित तकनीक सबस्ट्रेट सतह बनावट के बावजूद समान, चिकनी पतली फिल्म देती है। स्कैनिंग इलेक्ट्रॉन माइक्रोस्कोप (SEM), परमाणु बल माइक्रोस्कोप (AFM), और ऑप्टिकल सतह प्रोफ़िलोमीटर के माध्यम से अध्ययन की गई जमा eC_3N_4 फिल्म, अपकेंद्रित गति के आधार पर सतह खुरदरापन में भिन्नता दिखाती है। प्रारंभ में, फिल्म कवरेज में सुधार होता है, और अपकेंद्रित की घूर्णी गति में वृद्धि के साथ सतह खुरदरापन कम हो जाता है, और घूर्णी गति में और वृद्धि के साथ सतह खुरदरापन थोड़ा बढ़ जाता है। $\text{TiO}_2/\text{eC}_3\text{N}_4$ फिल्मों के प्रकाश विद्युत रासायनिक (PEC) अध्ययन, जिसमें लीनियर स्वीप वोल्टमैट्री (LSV) और इलेक्ट्रोकेमिकल इम्पेडेंस स्पेक्ट्रोस्कोपी (EIS) शामिल हैं, का कहना है कि सेंट्रीफ्यूज

तकनीक स्पिन कोटिंग तकनीक की तुलना में बेहतर हेटेरोजंक्शन बनाती है, जो कि PEC वॉटर स्प्लिटिंग को बढ़ाती है।

C_3N_4 पतली फिल्मों को जमा करने में एक विलायक के उपयोग को खत्म करने के प्रयास में, एक नया तरीका, जो कि रेडियो आवृत्ति मैग्नेट्रॉन (RFM) के माध्यम से स्पटरिंग लक्ष्य के रूप में gC_3N_4 का उपयोग करके stoichiometric C_3N_4 पतली फिल्मों को जमा करता है, का पता चला है। पतली फिल्मों के नमूने अलग-अलग अवधि के लिए प्लाज्मा मीडिया के रूप में Ar और N_2 के तहत विभिन्न सबस्ट्रेट पर जमा किए जाते हैं। इन नमूनों का विश्लेषण SEM, ट्रांसमिशन इलेक्ट्रॉन माइक्रोस्कोपी (TEM), AFM, एक्स-रे विवर्तन विश्लेषण (XRD), एक्स-रे फोटोइलेक्ट्रॉन स्पेक्ट्रोस्कोपी (XPS), फोटोल्यूमिनेशन स्पेक्ट्रोस्कोपी (PL), और रमन स्पेक्ट्रोस्कोपी द्वारा किया जाता है। PEC अध्ययन, जिनमें कटा हुआ प्रकाश वोल्टमेट्री, आपतित फोटोन-से-विद्युत धारा रूपांतरण दक्षता और EIS भी शामिल हैं, RFM स्पटरिंग तकनीक के माध्यम से गठित TiO_2/C_3N_4 हेटेरोजंक्शन नमूनों पर किये गए हैं। प्लाज्मा माध्यम के रूप में Ar का उपयोग TiO_2/C_3N_4 हेटेरोजंक्शन नमूना में stoichiometrically रूढ़िवादी C_3N_4 की एक पतली फिल्म के गठन की अनुमति देता है। PEC और PL अध्ययनों ने निष्कर्ष निकाला कि Ar प्लाज्मा के तहत गठित TiO_2/C_3N_4 हेटेरोजंक्शन ने N_2 प्लाज्मा द्वारा गठित TiO_2/C_3N_4 हेटेरोजंक्शन की तुलना में उच्च विद्युत धारा घनत्व और कम प्रतिबाधा की पेशकश की। यह स्पटरिंग प्रक्रिया में लक्ष्य के रूप में ग्रेफाइट के साथ N_2 गैस प्रवाह दर को नियंत्रित करने में कठिनाई के बिना एक stoichiometric और प्रकाश सक्रिय C_3N_4 की पतली फिल्म बनाने के लिए स्पटरिंग लक्ष्य के रूप में संपीड़ित C_3N_4 के लाभकारी उपयोग को दर्शाता है। इसके अलावा, स्पटरिंग प्रक्रिया को पतली फिल्म निर्माण के लिए किसी फैलाव की आवश्यकता नहीं होती है, और इसलिए पतली फिल्म निर्माण में विलायक की आवश्यकता समाप्त हो जाती है।

सब्सट्रेट TiO₂ नैनोस्ट्रक्चर और सेंसिटाइज़र C₃N₄ पतली फिल्मों के बीच संपर्क क्षेत्र को बढ़ाने के लिए, TiO₂ के एक नए विवृत शाखित नैनोकॉस्ट्रक्चर को संश्लेषित किया गया है। TiO₂ पत्री पर तने से जुड़े हुए TiO₂ नैनोफ्लावर सरणी को हाइड्रोजन पेरोक्साइड और हाइड्रोफ्लोरोइक एसिड विलयन द्वारा 80 °C पर टाइटेनियम के उष्मरासायनिक पाचन द्वारा संश्लेषित किया जाता है। TiO₂ नैनोफ्लावर में एनाटेज़ TiO₂ शामिल है, जो TEM, XRD, XPS आधारित डेपथ प्रोफाइल, और ऊर्जा फैलाने वाले एक्स-रे आधारित तात्विक मानचित्रण (Energy dispersive X-ray based elemental mapping) के अनुसार Ti धातु कोर को घेरे हुए है। वायु annealed नमूनों के भौतिक विश्लेषण ने लगभग 35 नैनोमीटर आकार के एनाटेज़ (101) और एनाटेज़ (200) क्रिस्टल की प्रमुख उपस्थिति को सत्यापित किया। पानी के विभाजन में TiO₂/C₃N₄ हेटेरोजंक्शन की फोटोएक्टिविटी का मूल्यांकन TiO₂ नैनोफ्लावर के साथ C₃N₄ द्वारा बनाई गई हेटेरोजंक्शन के लिए किया गया था, और इसकी तुलना TiO₂ नैनोट्यूबलर सरणी के साथ C₃N₄ द्वारा बनाई गई हेटेरोजंक्शन से की जाती है। LSV और EIS से यह पाया गया कि उष्मरासायनिक पाचन द्वारा संश्लेषित तने से जुड़े हुए TiO₂ नैनोफ्लावर सरणी द्वारा गठित TiO₂/C₃N₄ हेटेरोजंक्शन, TiO₂ नैनोट्यूब सरणी द्वारा गठित TiO₂/C₃N₄ हेटेरोजंक्शन की तुलना में पानी के विभाजन की दिशा में बेहतर PEC गतिविधि प्रदान करता है। उष्मरासायनिक पाचन विधि के अपशिष्टों से खर्च किए गए हाइड्रोफ्लोरोइक एसिड की पुनः प्राप्ति की एक विधि की भी पहचान की गई है।

Contents

Chapter 1. Introduction	1
1.1. Hydrogen generation by catalytic processing of fossil fuels	1
1.1.1. Steam methane reforming	1
1.1.2. Partial oxidation of fossil fuels	2
1.1.3. Coal gasification	2
1.2. Hydrogen generation from biomass	3
1.3. Hydrogen generation by water splitting	3
1.3.1. Water electrolysis	3
1.3.2. Thermochemical water splitting	5
1.3.3. Water biophotolysis	6
1.3.4. Water photolysis	6
1.3.5. Photoelectrochemical water splitting	9
1.3.6. Other techniques for water splitting	10
1.4. PEC water splitting – the process of choice	10
1.5. The motivation for the thesis	12
1.6. Scope and objectives of the thesis	14
1.7. Organization of the thesis	15
Chapter 2. Literature Review	16
2.1. Energetics of PEC water splitting	16
2.2. Process steps of PEC water splitting	16
2.2.1. Photon absorption and exciton generation	16
2.2.2. Charge separation and carrier transport	17
2.2.3. Interfacial charge transport and product formation	18
2.2.4. Product management	18
2.3. Configuration of the PEC water splitting cell	19
2.3.1. Electrolyte	20
2.3.2. Counter Electrode (CE)	21
2.3.3. Working Electrode (WE)	21
2.3.3.1. Titanium dioxide (TiO ₂)	22
2.3.3.2. Graphitic carbon nitride (gC ₃ N ₄)	23
2.3.3.3. Problems with different photoelectrode materials	24
2.4. Remedial approaches to enhance the photoelectrode efficiency	24
2.4.1. Sensitization through the formation of heterojunctions	25
2.4.1.1. Fabrication of heterojunctions through sensitization by wet methods	26

2.4.1.2.	<i>Fabrication of heterojunctions through sensitization by dry methods</i>	27
2.4.2.	<i>Nanostructuring of photoelectrode materials</i>	28
Chapter 3. Experimental Methods		30
3.1.	<i>Synthesis and fabrication methods</i>	30
3.1.1.	<i>Synthesis of TiO₂ nanotubular array through anodization method</i>	30
3.1.2.	<i>Synthesis of TiO₂ nanoflower structure through thermochemical method</i>	31
3.1.2.1.	<i>Recovery of spent fluorides</i>	31
3.1.3.	<i>Synthesis of C₃N₄ thin film through centrifugation method</i>	31
3.1.3.1.	<i>Synthesis of gC₃N₄</i>	31
3.1.3.2.	<i>Synthesis of the exfoliated form of gC₃N₄ (eC₃N₄)</i>	32
3.1.3.3.	<i>Assembly of eC₃N₄ thin film through centrifugation method</i>	32
3.1.4.	<i>Synthesis of C₃N₄ thin film through the RFM sputtering method</i>	33
3.1.4.1.	<i>Fabrication of the RFM sputtering target</i>	33
3.1.4.2.	<i>Deposition of the thin films</i>	33
3.2.	<i>Sample nomenclature</i>	34
3.3.	<i>Characterization methods</i>	35
3.3.1.	<i>Physical Characterization</i>	36
3.3.1.1.	<i>Scanning Electron Microscopy (SEM)</i>	36
3.3.1.2.	<i>Transmission Electron Microscopy (TEM)</i>	36
3.3.1.3.	<i>Atomic Force Microscopy (AFM)</i>	37
3.3.1.4.	<i>Optical Surface Profile (OSP)</i>	37
3.3.1.5.	<i>Dynamic Light Scattering (DLS)</i>	37
3.3.1.6.	<i>Fourier Transformed Infra-Red spectroscopy (FTIR)</i>	38
3.3.1.7.	<i>Energy Dispersive X-ray Spectroscopy (EDX)</i>	38
3.3.1.8.	<i>Raman Spectroscopy (Raman)</i>	39
3.3.1.9.	<i>X-ray Photoelectron Spectroscopy (XPS)</i>	39
3.3.1.10.	<i>X-ray Diffraction Analysis (XRD)</i>	40
3.3.1.11.	<i>Photo-Luminescence Analysis (PL)</i>	40
3.3.2.	<i>PEC Characterization</i>	41
3.3.2.1.	<i>Electrode preparation</i>	41
3.3.2.2.	<i>Experimental setup</i>	42
3.3.2.3.	<i>Linear Sweep Voltammetry (LSV)</i>	43
3.3.2.4.	<i>Chopped Light Voltammetry (CLV)</i>	44
3.3.2.5.	<i>Chronoamperometry (CA)</i>	44
3.3.2.6.	<i>Electrochemical Impedance Spectroscopy (EIS)</i>	44

Chapter 4. Thin Film like Assembly of Exfoliated C_3N_4 Nanoflakes by a Solvent Non-Evaporative Method Using Centrifuge	46
4.1. Results and Discussion	46
4.1.1. Characterization of the eC_3N_4 nanoflakes	46
4.1.2. Characterization of the eC_3N_4 suspension	47
4.1.3. Formation of the eC_3N_4 thin film assembly	48
4.1.4. PEC activity of the fabricated TiO_2/eC_3N_4 heterojunctions	56
Chapter 5. Formation of C_3N_4 Thin Films through the Stoichiometric Transfer of the Bulk Synthesized gC_3N_4 using RFM Sputtering	59
5.1. Results and Discussion	59
5.1.1. Film Growth	59
5.1.2. Film Composition	62
5.1.3. PEC and Optical characterization	66
5.1.4. Film Thickness Optimization	69
5.1.5. C_3N_4 Film Formation – Reactive vs. Stoichiometric Sputtering	71
Chapter 6. A Thermochemical Method of Synthesizing Stemmed TiO_2 Nanoflower Structures for TiO_2/C_3N_4 Heterojunctions with Enhanced Solar Water splitting	73
6.1. Results and Discussion	73
6.1.1. Structural Characterization	73
6.1.2. Compositional Characterization	76
6.1.3. PEC characterization	80
6.1.4. Recovery of spent HF	83
6.1.5. The growth of the TiO_2 nanostructure	85
Chapter 7. Summary and Conclusions	88
7.1. Summary	88
7.2. Conclusions	88
7.3. Future Scope	91
Chapter 8. Appendix	94
8.1. Regarding formation of C_3N_4 thin films by RFM sputtering based methods	94
8.1.1. SEM micrograph of the deposited thin film samples TFA4 and TFN4	94
8.1.2. SEM-EDX based Elemental mapping	95
8.1.3. Nuclear Magnetic Resonance (NMR) study of the synthesized gC_3N_4	95
8.1.4. Photoluminescence (PL) and Time-resolved PL (TRPL) studies	96
8.1.5. CA analysis of RFM sputtering deposited thin film-based heterojunctions	97
8.1.6. PEC study of TiO_2/CN_x heterojunction HCNX	98
8.2. Regarding synthesis of TiO_2 nanostructures	98

8.2.1.	<i>HRTEM micrograph of TiO₂ nanotubular array sample NT</i>	98
8.2.2.	<i>SEM micrograph of the TiO₂ nanotubular array sample NT</i>	99
8.2.3.	<i>XRD analysis of TiO₂ nanotubular array sample NT</i>	99
8.2.4.	<i>Effect of the thermochemical digestion conditions on growth of TiO₂ nanoflowers</i>	100
8.2.5.	<i>HRTEM micrograph of TiO₂ nanoflower sample NF</i>	104
8.2.6.	<i>Comparison with recent studies on TiO₂/C₃N₄ heterojunctions</i>	105
8.2.7.	<i>Faradaic efficiency calculations</i>	106
8.2.8.	<i>CA analysis of TiO₂ nanoflower based heterojunction NFH</i>	107
Chapter 9.	<i>References</i>	110

List of Abbreviations

Abbreviation	Expansion
Z	Modulus of electrochemical impedance
AC	Alternating current
AFM	Atomic force microscopy
BET	Brunauer-Emmett-Taylor
CA	Chrono-amperometry
CB	Conduction band
CE	Counter electrode
CHNSO	Carbon Hydrogen Nitrogen Sulphur Oxygen (analyzer)
CLV	Chopped light voltammetry
DC	Direct current
DI Water	De-ionized water
DLS	Dynamic light scattering
eC ₃ N ₄	Exfoliated carbon nitride
EDX	Energy dispersive x-ray (spectroscopy)
EHR	Electron-hole recombination
EIS	Electrochemical impedance spectroscopy
FESEM	Field emission scanning electron microscopy
FTIR	Fourier transformed infra-red (spectroscopy)
gC ₃ N ₄	Graphitic carbon nitride

HER	Hydrogen evolution reaction
HRTEM	High-resolution transmission electron microscopy
$\text{Im} Z $	Imaginary part of the electrochemical impedance
IPCE	Incident photon-to-current conversion efficiency
IR	Infra-red
LSV	Linear sweep voltammetry
LVW	London Van der Waals
NF	Nanoflower (nanostructure of TiO_2)
NHE	Normal hydrogen electrode
NMR	Nuclear magnetic resonance (spectroscopy)
NT	Nanotubes (nanostructure of TiO_2)
OER	Oxygen evolution reaction
OSP	Optical surface profile
PEC	Photoelectrochemical
PL	Photo luminescence
R_a	Averaged surface roughness
Raman	Raman spectroscopy
RE	Reference electrode
$\text{Re} Z $	Imaginary part of the electrochemical impedance
RFM	Radio frequency magnetron (sputtering)
RHE	Reversible hydrogen electrode

rpm	Revolutions per minute (rotation speed)
SAED	Selected area electron diffraction
SEM	Scanning electron microscopy
SHE	Standard hydrogen electrode
SMR	Steam methane reforming
SRF	Surface roughness factor
STP	Standard temperature and pressure
TEM	Transmission electron microscopy
TRPL	Time-resolved photo luminescence
VB	Valence band
WE	Working electrode
XPS	X-ray photoelectron spectroscopy
XRD	X-ray diffraction

List of Figures

- Fig. 1.1** *Schematic representation of thermochemical water splitting process, q_r represents heat input from all sources at temperature T_r , and W_i represents useful work input, and q_0 represents waste heat rejected to the sink at temperature T_0 , reproduced with permission [1]* 5
- Fig. 1.2** *Schematic representation of photocatalytic water splitting process* 8
- Fig. 1.3** *Schematic representation of a PEC full cell* 12
- Fig. 1.4** *Schematic representation of the most significant problems of the PEC electrodes and their solutions (problems are shown by red font color, solutions are shown by green font color, and intermediate choices are marked in blue font color), based on Chen et al. [69]* 13
- Fig. 2.1** *General schematics of (a) Anodic half-cell, (b) Cathodic half-cell, and (c) PEC full cell* 19
- Fig. 2.2** *Comparison of different photoelectrode materials with HER and OER potentials based on the conduction and valence band energy levels, dotted lines mark the HER (H_2O/H_2 , 0.0 V vs. NHE) and OER (O_2/H_2O , +1.23 V vs. NHE) potentials, reproduced with permission [76]* 22
- Fig. 2.3** *(a) Three types of heterojunctions, (b) TiO_2/gC_3N_4 heterojunction, an example of type-II heterojunction and spectral sensitization* 25
- Fig. 3.1** *Typical photoelectrode specimen and a representative scale* 41

Fig. 3.2	<i>(a) Schematic diagram and (b) actual image of the PEC experimental setup and, (c) representative image of the PEC cell used in the present work</i>	42
Fig. 4.1	<i>HRTEM image of exfoliated C_3N_4 nanoflake used in the study (scale bar reads 20 nm)</i>	46
Fig. 4.2	<i>FTIR spectrum of the gC_3N_4 powder used for synthesis of eC_3N_4 through exfoliation</i>	47
Fig. 4.3	<i>DLS based particle size distribution in the original eC_3N_4 suspension and the solvent</i>	48
Fig. 4.4	<i>(a) FESEM image of sample 8k, (b) AFM image of sample 8k, (c) FESEM image of sample 16k, (d) AFM image of sample 16k, (e) FESEM image of sample 24k, (f) AFM image of sample 24k, (g) FESEM image of sample 32k, (h) AFM image of sample 32k, (i) FESEM image of sample SpinC, (j) AFM image of sample SpinC</i>	49
Fig. 4.5	<i>Optical surface profiles of bare glass substrate, samples 8k, 16k, 24k, 32k, and SpinC</i>	54
Fig. 4.6	<i>LSV based comparison of PEC activities of TiO_2/eC_3N_4 heterojunctions formed at different centrifugation speeds and by spin coating technique</i>	57
Fig. 4.7	<i>EIS-Nyquist plot-based comparison of PEC activities of TiO_2/eC_3N_4 heterojunctions</i>	57
Fig. 4.8	<i>EIS-Nyquist plot (high frequencies, 100 kHz to 100 Hz) of various heterojunctions</i>	58
Fig. 5.1	<i>HRTEM images of samples (a) TFA4, (b) TFN4</i>	59
Fig. 5.2	<i>OSP measured thicknesses and fitted line for the deposited film samples TFAt and TFNt ($t = 0.5, 1, 2, 4, \text{ and } 6 \text{ h}$)</i>	60

Fig. 5.3	<i>AFM images of samples (a) TFA4, (b) TFN4, (c) bare borosilicate glass substrate, and (d) BET measurement based N₂ adsorption-desorption plots for samples TFA4, TFN4, and porous Carbon fiber-based substrate</i>	61
Fig. 5.4	<i>(a) FTIR spectra (b) Raman spectra, and (c) XRD pattern of thin films deposited as samples TFA4 and TFN4</i>	63
Fig. 5.5	<i>XPS based survey and elemental spectra of C 1s and N1s for samples (a-c) gC₃N₄ target material, (d-f) sample TFA4, and (g-i) sample TFN4</i>	65
Fig. 5.6	<i>(a) CLV, (b) IPCE, (c) Steady-state PL, and (d) TRPL plots of TiO₂/C₃N₄ heterojunction samples HTFA4 and HTFN4</i>	67
Fig. 5.7	<i>(a) Nyquist and (b) Bode plot of EIS data of the heterojunctions HTFA4 and HTFN4; EIS data fitted with equivalent circuits for the heterojunctions (c) HTFA4, (d) HTFN4</i>	68
Fig. 5.8	<i>(a) CLV and (b) Steady-state PL study of the TiO₂ substrate-based heterojunction samples HTFA_t (t = 1, 2, 3, and 4h)</i>	70
Fig. 5.9	<i>SEM images showing coverage of the TiO₂ nanotubular arrays during formation of the heterojunction samples HTFA_t (t = 1, 2, 3, and 4h) (a) bare TiO₂ nanotubular array-based substrate, (b) Sample HTFA1, (c) Sample HTFA3, and (d) Sample HTFA4; the scale bar reads 200 nm for (a), (b), and (c) and 300 nm for (d)</i>	71
Fig. 6.1	<i>FESEM image of (a) TiO₂ nanostructure prepared using 30% H₂O₂ and (b) TiO₂ nanoflower prepared using 100 mM HF in 30% H₂O₂</i>	73
Fig. 6.2	<i>Similarity between TiO₂ nanoflowers obtained by thermochemical synthesis and natural flowers, (a) and (c) FESEM images of the prepared TiO₂ nanoflower samples, (b) White Rain Lily [188] and (d) Fire-pot Dahlia [189]</i>	74

Fig. 6.3	<i>HRTEM images of NF, (a) a complete nanoflower, (b) flower petal, (c) zoomed view of the flower petal (d) SAED diffractogram</i>	75
Fig. 6.4	<i>XRD pattern of the TiO₂/C₃N₄ heterojunction samples NFH and NTH</i>	76
Fig. 6.5	<i>SEM-EDX based elemental mapping of sample NF of TiO₂ (scale 10 μm)</i>	77
Fig. 6.6	<i>(a) Ti 2p XPS spectra of sample NF of TiO₂, (b) O 1s XPS spectra of sample NF of TiO₂</i>	78
Fig. 6.7	<i>Current density comparison of NTH and NFH based on LSV</i>	81
Fig. 6.8	<i>(a) EIS based Nyquist plot for comparison of PEC activities of NTH and NFH, (b) EIS based Bode plot for comparison of PEC activities of NTH and NFH</i>	81
Fig. 6.9	<i>(a) SEM micrograph of the recovered CaF₂ in its powdered form, (b) SEM-EDX elemental mapping and XRD diffractogram of the recovered CaF₂</i>	84
Fig. 6.10	<i>(a) FESEM micrograph of eC₃N₄ coated TiO₂ nanotubes, (b) schematic representation of eC₃N₄ coated TiO₂ nanotubes, (c) FESEM micrograph of eC₃N₄ coated stemmed nanoflower like nanostructure of TiO₂, and (d) schematic representation of eC₃N₄ coated stemmed nanoflower of TiO₂</i>	87
Fig. 7.1	<i>Schematic representation of laterally placed different heterojunction and utility as multifunctional photoelectrode</i>	93
Fig. 8.1	<i>SEM images of the specimens of the thin films from samples (a) TFA4 and (b) TFN4</i>	94

Fig. 8.2	<i>SEM-EDX based elemental mappings of samples of (a) thermochemically synthesized gC₃N₄ powder, (b) TFA4, and (c) TFN4</i>	95
Fig. 8.3	<i>Solid-state ¹³C NMR spectrum for the gC₃N₄ powder, synthesized from dicyandiamide by thermal polycondensation method and used to fabricate the sputtering target</i>	96
Fig. 8.4	<i>TRPL study of thin films samples HTFA4 and HTFN4, excitation at 377 nm and response monitored at 620 nm wavelength</i>	96
Fig. 8.5	<i>PL study of thin films samples deposited under Ar and N₂ for different RFM sputtering powers (a) samples prepared using Ar and (b) samples prepared using N₂</i>	97
Fig. 8.6	<i>CA based stability study (0.9 V vs. Ag/AgCl in saturated KCl) of the heterojunction samples HTFA4 and HTFN4</i>	97
Fig. 8.7	<i>PEC study of the heterojunction formed by the CN_x thin film deposited on TiO₂ substrate by sputtering the graphite target at 100 W RFM power, under 40 sccm N₂ flow, for 4 h, (a) LSV plot under dark and illuminated conditions and (b) Nyquist plot of EIS at 0 V under dark and illuminated conditions</i>	98
Fig. 8.8	<i>HRTEM image of TiO₂ nanotubular array-based sample NT (scale bar reads 20 nm)</i>	98
Fig. 8.9	<i>FESEM image of the anodized nanotubular structure of TiO₂, scale bar reads 300 nm</i>	99
Fig. 8.10	<i>XRD pattern of the anodized nanotubular structure NT of TiO₂</i>	99
Fig. 8.11	<i>FESEM image of samples (a) 0_NF008_60, (b) 3_NF008_60, (c) 5_NF008_60, (d) 0_NF100_60, (e) 3_NF100_60, (f) 5_NF100_60, (g) 0_NF500_60, (h) 3_NF500_60 and (i) 5_NF500_60 nanostructures of TiO₂ that evolved during</i>	101

thermochemical digestion in the presence of different concentrations of H₂O₂ and HF (refer table 8.1)

- Fig. 8.12** *FESEM image of samples (a) 3_NF008_12, (b) 3_NF008_24, (c) 3_NF008_60, (d) 3_NF100_12, (e) 3_NF100_24, (f) 3_NF100_60, (g) 3_NF500_12, (h) 3_NF500_24 and (i) 3_NF500_60 nanostructures of TiO₂ that evolved during thermochemical digestion in the presence of 30% H₂O₂ and different concentrations of HF (refer table 8.1)* 102
- Fig. 8.13** *HRTEM micrographs of TiO₂ nanoflower sample NF (a) and (b) show two overlapping petals, (c) and (d) show oxide layer covering the inner core (scale bars read 5 nm)* 104
- Fig. 8.14** *(a) Gas chromatogram of the gas specimen collected from NFH in anodic half-cell, (b) Gas chromatogram of the gas specimen collected from NTH in anodic half-cell* 106
- Fig. 8.15** *CA plot for heterojunction NFH, performed at 0.23 V vs. Ag/AgCl in saturated KCl* 107
- Fig. 8.16** *An illustration of the approach of the lightest particles during the centrifuge-based thin film assembly of eC₃N₄* 108

List of Tables

Table 3.1	<i>Sample nomenclature of the thin film specimens deposited using the centrifuge-based thin film deposition method</i>	34
Table 3.2	<i>Nomenclature and preparation parameters of the thin film samples prepared by stoichiometric transfer of C_3N_4 using RFM sputtering</i>	35
Table 5.1	<i>Value of the fitted parameters of the equivalent circuit of EIS data</i>	69
Table 8.1	<i>Summary of observations from FESEM images of various digested Ti foil samples</i>	103
Table 8.2	<i>Comparison of present work with recent studies</i>	105